

## Chapter 3: Atmospheric implications of sulfur isotope effects on the ultraviolet absorption spectrum of carbonyl sulfide\*

### 3.1 Introduction

The relative enrichment of N<sub>2</sub>O isotopologues (<sup>14</sup>N<sup>14</sup>N<sup>16</sup>O, <sup>14</sup>N<sup>15</sup>N<sup>16</sup>O, <sup>15</sup>N<sup>14</sup>N<sup>16</sup>O and <sup>14</sup>N<sup>14</sup>N<sup>18</sup>O) in the stratosphere has been attributed to the relative differences in the UV photolysis rates [Miller and Yung, 2000]. Isotopic effects were explained as the consequence of among the zero point energies (ZPEs) of the ground states of the various isotopologues. In this case, the absorption spectra of the heavier N<sub>2</sub>O isotopologues are blue-shifted relative to that of <sup>14</sup>N<sup>14</sup>N<sup>16</sup>O [Miller and Yung, 2000], and thus photolysis at wavelengths longer or shorter than  $\lambda_{\max}$  should result in the enrichment or depletion, respectively, of the heavier isotopologues in the remaining material.

Recent experiments showed that the actual enrichment factor during the photolysis of N<sub>2</sub>O at 205 nm ( $\lambda_{\max} = 185$  nm) is in fact considerably larger than the value predicted by Miller and Yung [Griffith *et al.*, 2000; Turatti *et al.*, 2000]. It was suggested that the discrepancy could be due to the involvement of bending hot bands. Bending circumvents the symmetry restrictions associated with dipole transitions connecting the linear ground state of 16 valence electron triatomics, such as N<sub>2</sub>O and OCS, with their bent excited states, and would enhance the Franck-Condon factors [Zhang *et al.*, 2000]. Detailed calculations on the electronic spectrum of N<sub>2</sub>O in yielded small, negative isotopic enrichment factors over the entire absorption band [Johnson *et al.*, 2001].

---

\* Adapted in part from Colussi, A.J., F.Y. Leung, and M.R. Hoffmann, Sulfur Isotope Effects on the Ultraviolet Absorption Spectrum of Carbonyl Sulfide. Atmospheric Implications, *Submitted for review*, 2002.

As detailed in Chapter 2, the analysis of high-resolution solar occultation FTIR spectra taken by the NASA/JPL MkIV instrument revealed that OC<sup>34</sup>S was increasingly depleted with altitude. The apparent isotopic enrichment factor  $\epsilon' \sim +73 \text{ ‰}$  associated with the depletion mechanism, led to the prediction that SSA originating from OCS should be highly enriched in <sup>34</sup>S [Leung *et al.*, 2002].

Although there are significant contributions from other loss mechanisms, namely oxidation by OH and O radicals, accounting for about 30% of the total, solar photolysis has been identified as the principal depletion mechanism.

A positive  $\epsilon'$  at  $\lambda \leq \lambda_{\text{max}} = 223 \text{ nm}$  is consistent with Miller and Yung's analysis. As a consequence, we were motivated to validate our results for OCS by directly comparing the absorption spectra of OC<sup>32</sup>S and OC<sup>34</sup>S as measured in the laboratory.

### 3.2 Experimental

The UV-Vis absorption spectra of OCS were recorded at room temperature with a Cary 480 UV-Vis spectrophotometer set to 0.08 nm resolution, using a 10 cm-long gas cell fitted with suprasil windows. The stability of the Cary 480 is  $\pm 0.04 \text{ nm}$ . The average of duplicate spectra are reported, although the results do not vary significantly among individual spectra.

OC<sup>32</sup>S (~90% pure, Aldrich), and 'enriched' OC<sup>34</sup>S (Icon Isotopes, see below) were used after purification.

Preliminary UV spectra of the raw OC<sup>32</sup>S and OC<sup>34</sup>S samples in the 200-300 nm range revealed significant contamination. OC<sup>32</sup>S was contaminated primarily by CS<sub>2</sub>,

whose spectrum displays a distinctive pattern below 220 nm [Molina *et al.*, 1981]. The spectrum of raw OC<sup>34</sup>S showed significant contamination by CS<sub>2</sub> and H<sub>2</sub>S.

H<sub>2</sub>S was removed as HgS by overnight treatment with Hg(II) sulfate solutions at pH = 1 in the dark. The remaining product was distilled three times at -135 °C under vacuum. The middle fraction was collected in each case. OC<sup>32</sup>S was treated in the same way.

GC-MS analysis (Hewlett-Packard 6890 GC/5973 MS column, 393 K) of the purified samples indicated that OC<sup>34</sup>S actually had a <sup>34</sup>S/<sup>32</sup>S ratio  $\rho = 0.833$ , and contained about 51% CO<sub>2</sub>, a species that cannot be separated by distillation at -135 °C. Since CO<sub>2</sub> is transparent between 200-260 nm and the recorded spectra were subsequently normalized, its presence is inconsequential. H<sub>2</sub>S and CS<sub>2</sub> impurities, which eluted at 5.0 and 11.6 min under present conditions, respectively, were both below the detection limit (less than 0.1%) in OC<sup>32</sup>S and OC<sup>34</sup>S chromatograms. No other species were present in the purified samples.

### 3.3 Results and discussion

The magnitude of the experimental random errors associated with gas pressure measurements (a few %) would normally exceed the precision required to reveal heavy-atom isotope effects (of the order of a few ‰ in  $\epsilon$ ). We minimized the influence of such errors by normalizing the areas under the OC<sup>34</sup>S and OC<sup>32</sup>S spectra.

Area conservation, a consequence of the Born-Oppenheimer approximation, only holds for transitions originating from single vibronic states. In principle, the potentially dissimilar hot band contributions to OC<sup>34</sup>S and OC<sup>32</sup>S spectra at room temperature would

make the comparison between their normalized spectra a compromise solution dealing with practical limits to precision. In fact, bending frequencies are so similar:  $\nu_2 = 528.86 \text{ cm}^{-1}$  in  $\text{OC}^{32}\text{S}$  vs.  $\nu_2 = 528.04 \text{ cm}^{-1}$  in  $\text{OC}^{34}\text{S}$  that area normalization is not expected to significantly affect our conclusions. There was some concern that the normalization would be an unrealistic compromise because the spectra do not go to zero at the high energy. However, temperature effects are weaker at high energy than at low energies [Molina *et al.*, 1981], so the introduced inaccuracy is expected to be minor.

The processed spectra of purified  $\text{OC}^{32}\text{S}$  and  $\text{OC}^{34}\text{S}$  samples shown in Figure 3.1 were generated from recorded absorbances,  $A(\lambda)$ , by setting them to zero absorbance at 260 nm, normalizing the areas under the resulting curves, and filtering the outcome using 1% kernel smoothing. Shape differences between the  $\text{OC}^{34}\text{S}$  and  $\text{OC}^{32}\text{S}$  spectra, as well as their diffuse vibronic structure are preserved by smoothing (Figure 3.1). Normalized absorbances are proportional to the corresponding absorption cross-sections,  $\sigma$ .

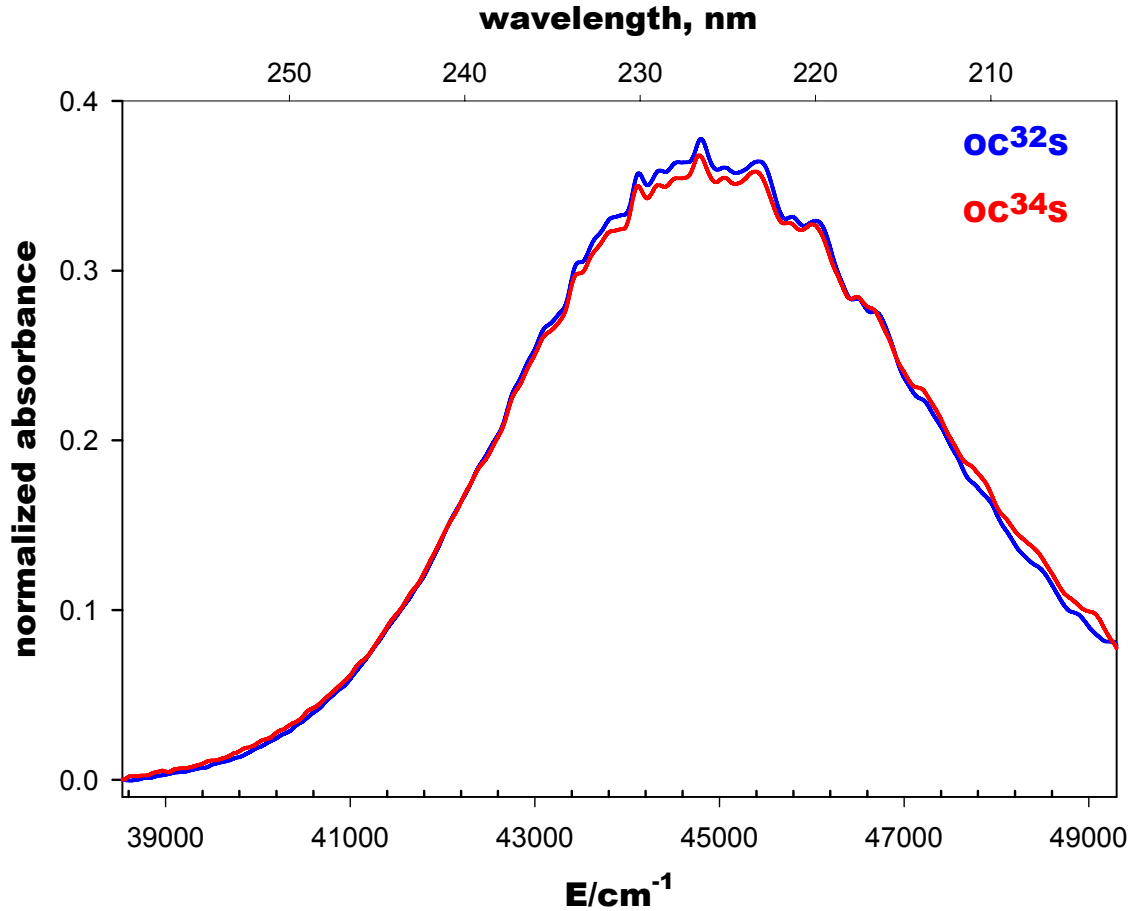


**Figure 3.1:** UV spectra of  $\text{OC}^{32}\text{S}$  and  $\text{OC}^{34}\text{S}$  at 666.6 Pa, 298 K.

To highlight the diffuse features present in the spectra of Figure 3.1 we fitted skewed Gaussians:

$$\varphi(\lambda) = a_0 + (a_1 + a_2\lambda)\exp[-(\lambda - a_3)^2/a_4] \quad (3.1)$$

to the unfiltered  $\sigma(\lambda)$  spectra. The smoothed differences between the unfiltered spectra and their continua:  $\sigma_{\text{diffuse}} = \sigma - \varphi$ , are shown in Fig. 3.2. This empirical procedure generates  $\sigma_{\text{diffuse}}$  spectra with a nearly flat baseline that allows for more direct comparison between the diffuse structure of both spectra. It is apparent that  $\text{OC}^{34}\text{S}$  spectrum is noticeably broader, particularly at high energies. Discrete features nearly overlap up to

about  $47,500 \text{ cm}^{-1}$ , above which both spectra lose coherence and display large isotope effects.

For the first-order photochemical decay of isotopologues A and B [ $A \equiv \text{OC}^{34}\text{S}$ , B  $\equiv \text{OC}^{32}\text{S}$ ]:

$$\frac{d[A]}{dt} = -k_a[A] \quad (3.2)$$

$$\frac{d[B]}{dt} = -k_b[B] \quad (3.3)$$

the isotopic fractionation ratio is defined as  $\alpha = k_A/k_B$ , and the isotopic enrichment factor as  $\varepsilon = \alpha - 1 = (k_A - k_B)/k_B = (\sigma_A - \sigma_B)/\sigma_B$ , where  $\sigma_A$  and  $\sigma_B$  are the monochromatic absorption cross sections. The last identity assumes isotope-independent quantum yields. The spectral dependence  $\varepsilon(\lambda)$  obtained from the normalized  $\text{OC}^{32}\text{S}$  and  $\text{OC}^{34}\text{S}$  spectra of Figure 3.1 is shown in Fig. 3.3, together with that calculated for a hypothetical  $\text{OC}^{34}\text{S}$  spectrum synthesized by blue-shifting the experimental  $\text{OC}^{32}\text{S}$  spectrum by the difference in the zero point energy ( the energy of the system where the vibrational quantum number  $v = 0$ ,  $E_0 = \frac{1}{2} h c \omega$ ) of the system

$$\Delta\text{ZPE} = \frac{1}{2} h \sum_{i=1}^3 ({}^{32}v_i - {}^{34}v_i) = 7 \text{ cm}^{-1} \quad (3.4)$$

between the  $\text{OC}^{32}\text{S}$  and  $\text{OC}^{34}\text{S}$  ground states, as proposed by Miller and Yung (2000). It is apparent that the agreement between the experimental and calculated  $\varepsilon(\lambda)$ 's is relatively poor.

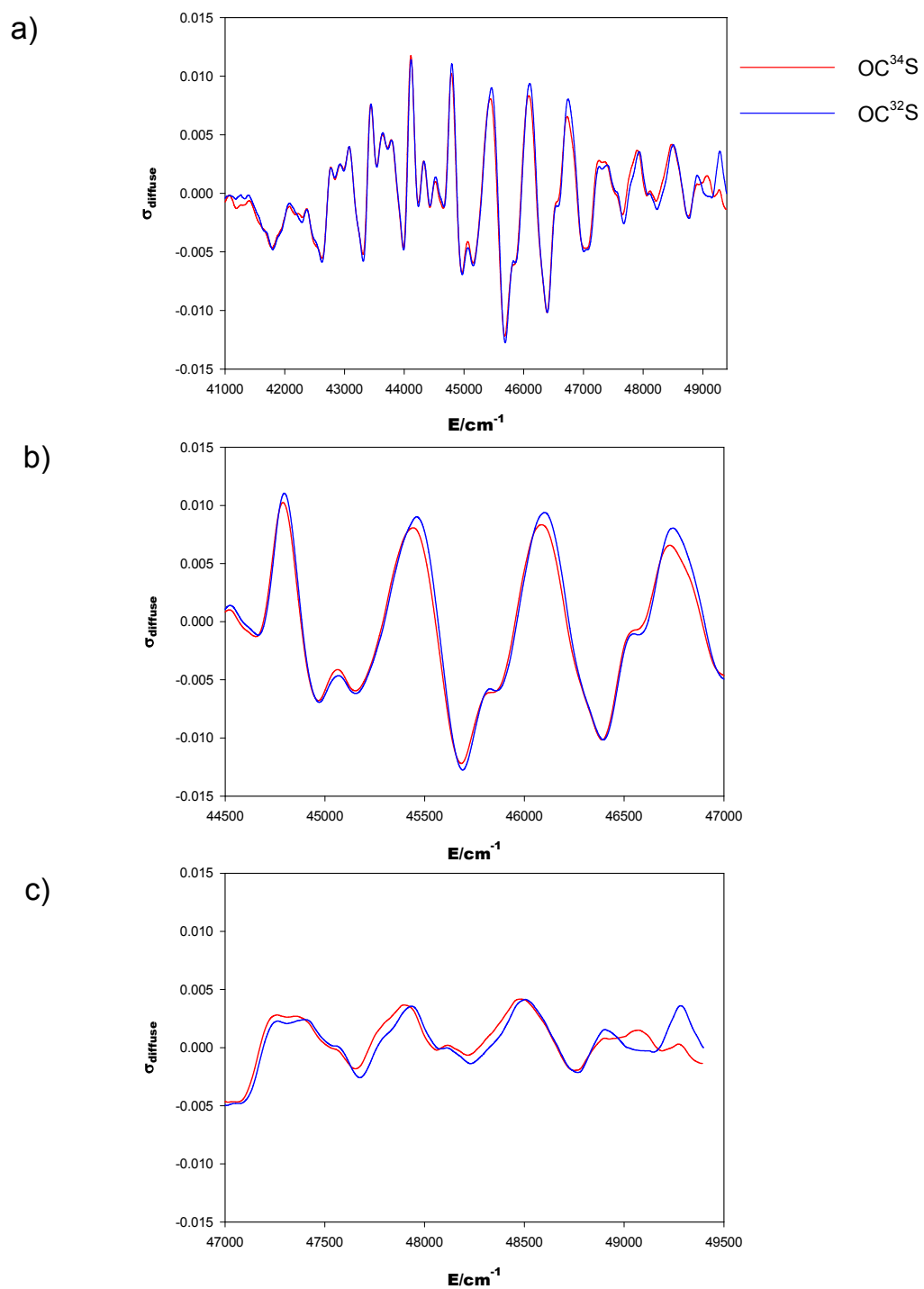


**Figure 3.2:** a) The diffuse structure of  $\text{OC}^{32}\text{S}$  and  $\text{OC}^{34}\text{S}$  UV spectra. The broad continua were subtracted from the spectra of Fig. 3.1. Expanded views in: b) between 44500 and 47000  $\text{cm}^{-1}$ . c) between 47000 and 49500  $\text{cm}^{-1}$ .

The experimental  $\varepsilon(\lambda)$  (Figure 3.3) is consistent with our previous findings of a high and positive value for the  $\varepsilon$  of OCS photolysis in the lower stratosphere. However, the reported  $\langle\varepsilon\rangle$  of  $\sim 73\%$  (Chapter 2) is an apparent enrichment factor, which is expected to be  $\sim 30\text{-}50\%$  lower than the actual enrichment factor of photolysis due to the effects of eddy diffusion [Rahn *et al.*, 1998], and which furthermore includes the isotopic effects from other, albeit not as important, OCS loss pathways. Moreover, the actual isotopic enrichment of OCS is dependent on the solar UV window, and therefore on altitude. If the behavior of  $\text{N}_2\text{O}$  is similar to that of OCS, temperature effects should be important. Molina *et al.* (1983) show that temperature effects on the UV spectrum of OCS is confined mainly to the red side of the absorption maximum. Nevertheless, low temperature experiments would clear up any ambiguity with regard to the temperature dependence of  $\varepsilon(\lambda)$ .

The relatively low experimental  $\varepsilon(\lambda)$  of  $\sim 73\%$  at 205 nm, at about the middle of the solar spectra, suggests that either there are significant experimental errors associated with our MkIV study, that there may be some error associated with area normalization of the  $\text{OC}^{32}\text{S}$  and  $\text{OC}^{34}\text{S}$  spectra, that the other OCS loss processes have significant associated isotopic enrichment factors, or that there are significant temperature effects on  $\varepsilon(\lambda)$ . However, it is difficult within the context of this work to determine which one or more of these factors accounts for the discrepancy between the spectral results reported here and the work in Chapter 2.

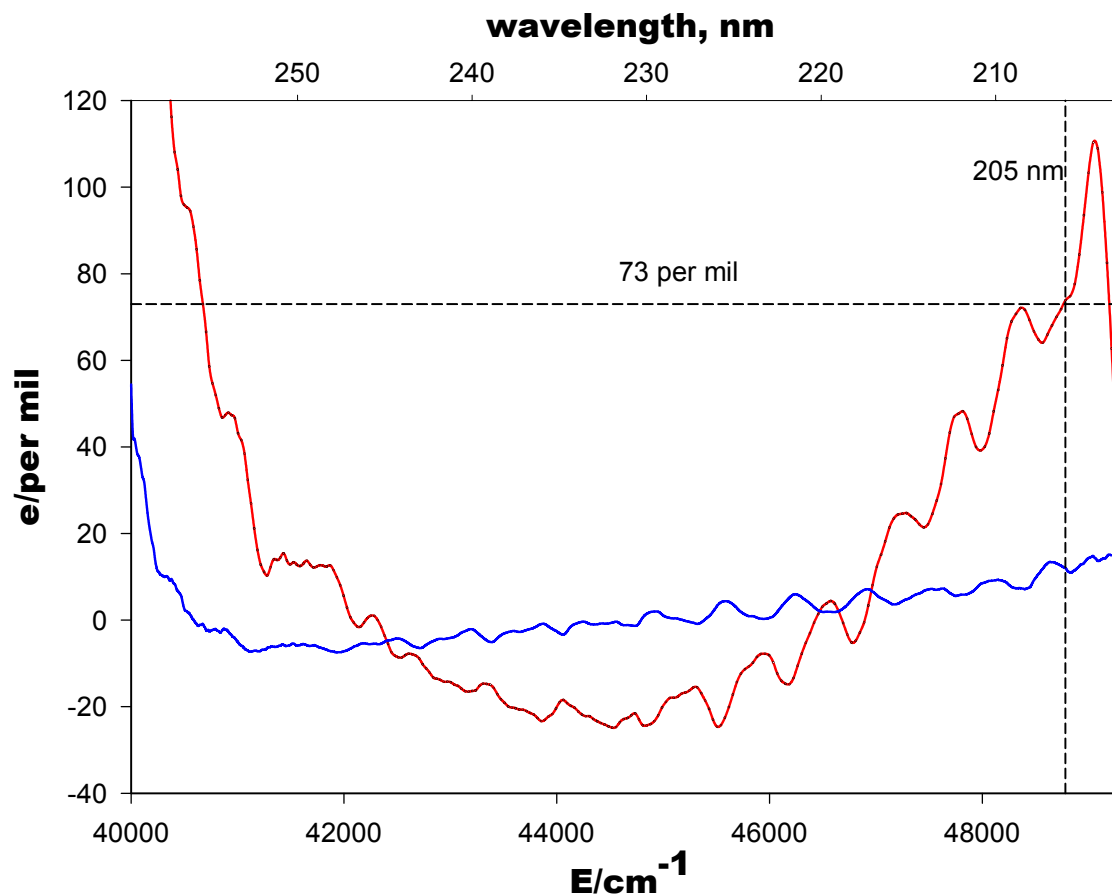


**Figure 3.3:** Red line: The experimental OCS sulfur isotopic enrichment factor  $\epsilon(\lambda)$  derived from the spectra of Fig. 1. Blue line:  $\epsilon(\lambda)$  calculated using M&Y's zero-point energy approximation. We obtain  $\epsilon = (73 \pm 10) \text{‰}$  at 205 nm, i.e., the products of OCS photolysis in the lower stratosphere are enriched in  $^{34}\text{S}$ .

While recent reports have shown that the simple theory of Miller and Yung (2000) has some deficiencies in attributing isotopic effects in the photodissociation of triatomics to the difference of the respective ZPE ground states [Griffith *et al.*, 2000; Johnson *et al.*, 2001; Zhang *et al.*, 2000], it is more difficult to identify the actual mechanism underlying our observations. Zhang *et al.*, (2000) suggested that discrepancies with the Miller and Yung model may arise from the dissimilarly populated hot bending bands of the various isotopologues/isotopomers. Hot bands are certainly involved in the temperature dependence of the OCS spectrum at  $\lambda \geq 220 \text{ nm}$  [Wu *et al.*,

1999], i.e., its role is expected to be confined to the red side of the spectral maximum. The small shift between the isotopologues bending frequencies (see above) will further minimize the influence of hot bands on  $\epsilon$  at 205 nm. Measurement of  $\text{OC}^{32}\text{S}$  and  $\text{OC}^{34}\text{S}$  absorption spectra over a broader range of temperatures could bracket even further the role of bending overtones.

It has been argued, by analogy with the spectra of diatomics, that the spatial contraction of the vibrational wavefunctions  $\Psi_{v=0}$ 's of the electronic ground state should narrow the absorption spectra of the heavier isotopologues [*Gordus and Bernstein*, 1954]. However, in a time dependent description the spectral width of the broad quasicontinuum actually reflects the dissociative lifetime of the excited wave packet [*Heller*, 1981; *Herzberg*, 1966]. On a purely repulsive upper state surface, kinematic effects could slow down the escape of the heavier system from the Franck-Condon region, resulting in a narrower continuum. However, if the escape were controlled by a diabatic crossing from the initially excited bound state(s) into the dissociative channel, crossing probabilities could be enhanced by lower velocities. Angular momentum conservation effects, via the larger moment of inertia of  $\text{OC}^{34}\text{S}$ , may also play a role in predissociation [*Herzberg*, 1966].

Dipole transitions from the  $^1\Sigma^+$  ground state of the 16 valence electron OCS molecule to its lowest-lying excited states  $^1\Sigma^-$  and  $^1\Delta$  are forbidden in the linear geometry by the strong selection rules  $\Delta\Lambda = \pm 1$  and  $+ \leftrightarrow -$  [*Suzuki et al.*, 1998]. The energy diagrams reported in that work are included here (Figures 3.4 and 3.5). In the bent geometry the  $^1\Delta$  state splits into  $A'$  and  $A''$  terms, while the  $^1\Sigma^-$  state becomes a  $A''$  term, all of which are accessible from  $^1\Sigma^+$  (X) via weakly allowed transitions. The lowest

dissociation channel  $\text{OCS}(X) + h\nu \rightarrow \text{S}(^1\text{D}_2) + \text{CO}(^1\Sigma^+)$  opens up at energies above 4.26 eV ( $\lambda \leq 290$  nm). The  $A'(^1\Delta)$  and  $A''(^1\Sigma^-)$  bound states can be populated by dipole transitions at  $\lambda \geq 200$  nm. The  $A'(^1\Delta)$  excited state is predissociatively stable, trapped by a  $\sim 0.7$  eV barrier located at  $R_{\text{C-S}} \sim 0.29$  nm. In the linear geometry, the  $^1\Delta$  state has a minimum at about  $R_{\text{C-S}} \sim 0.23$  nm, and crosses a repulsive  $^1\Pi$  state at about  $R_{\text{C-S}} \sim 0.25$  nm [Sugita *et al.*, 2000; Suzuki *et al.*, 1998]. This crossing is avoided in the bent geometry, however, becoming a conical intersection that leads to adiabatic dissociation via  $A'(^1\Pi)$  and  $A''(^1\Pi)$  states. The  $A'(^1\Delta)$  state also displays an avoided crossing with the  $^1\Sigma^+(X)$  state in the bending coordinate at about  $60^\circ$ , which also induces dissociation in the singlet manifold. The probability of curve crossing defines the escape lifetime from the Franck-Condon region, i.e., the width of the spectral continuum background, as well as the intensity of the diffuse features associated with the recurrences of the trapped trajectories.

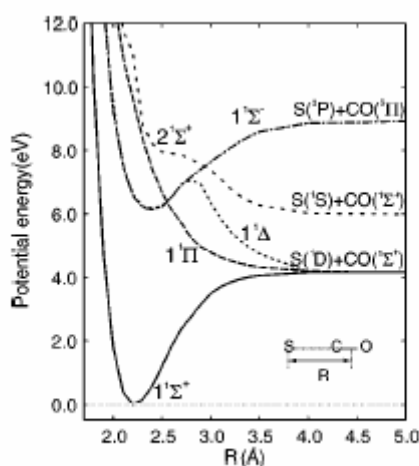


**Figure 3.4:** Potential energy curves as a function of the reaction coordinate in the linear geometry;  $r_{\text{CO}}$  is fixed at 1.13 Å. Figure is adapted from Suzuki *et al.* (1998).

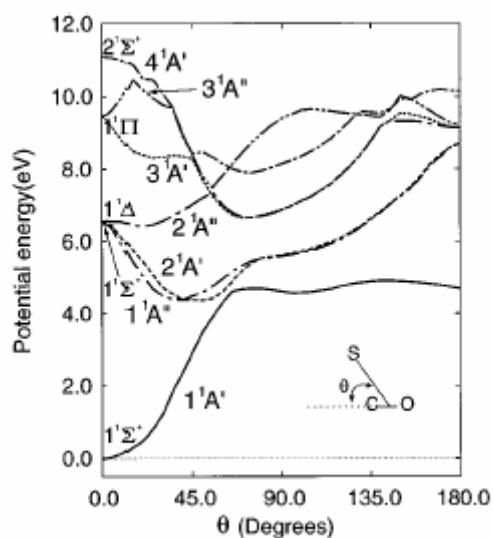


**Figure 3.5:** Potential energy curves as a function of the bending angle  $\theta$ ;  $R$  is fixed at 2.2 Å and  $r_{CO}$  at 1.13 Å. Figure is adapted from Suzuki et al. (1998).

The weak features noticeable in the OCS spectrum (Figure 3.2) formally correspond to  $710 \pm 20$  and  $650 \pm 15 \text{ cm}^{-1}$  progressions whose band intensities are nearly independent of temperature, and another set of  $520 \pm 20 \text{ cm}^{-1}$  spacings, that correspond to  $v_2$  hot bands that fade upon cooling [Breckenridge and Taube, 1970]. These bands can be alternatively interpreted as manifestations of the periodic motions of the wave packets trapped in the Franck-Condon basin [Flothmann et al., 1997; Kulander et al., 1991; Schinke and Engel, 1990], or as vibrations along the normal coordinate of the symmetric stretch [Flothmann et al., 1997; Pack, 1976]. Since  $710 \text{ cm}^{-1}$  corresponds to the stretching frequency of a highly perturbed half C-O bond (viz.  $2080 \text{ cm}^{-1}$  in ground state OCS), and since vibrationally cold CO ( $v' = 0, 1$ ) is produced in the photodissociation of OCS [Suzuki et al., 1998], few wave packets undergo delayed dissociation. According to this view the broader continuum (Fig. 3.2) and weaker sub-bands of the  $OC^{34}S$  spectrum relative to  $OC^{32}S$  (Fig. 3.2) are complementary manifestations of an inverse isotope effect

on the probability of first escape from the Franck-Condon basin. The solution of a time-dependent Schroedinger equation on the PES manifold of OCS could help settle this issue.

As noted previously, our measurements were taken at room temperature, and that stratospheric temperatures are about 100 K lower, and the effects of temperature may be significant.

### 3.4 Conclusions

We report positive values for the wavelength-dependent  $\epsilon(\lambda)$  over stratospherically relevant wavelengths based on the experimental UV spectra of OC<sup>32</sup>S and OC<sup>34</sup>S. This result supports the large, positive value found in Chapter 2 for the processing of OCS in the lower stratosphere. However, because the result from Chapter 2 also includes the isotopic effects of other OCS loss processes, it is difficult to directly compare the two results. Moreover,  $\epsilon_{\text{photolysis}}$  will vary with altitude because the intensity of solar radiation at any given wavelength is altitude dependent.

The spectral dependence  $\epsilon(\lambda)$  in the 200-260 nm range seems to be due to mass effects on OCS excited state(s) dynamics, rather than on equilibrium properties of its ground state.

**Acknowledgements.** Special thanks to Kyle Bayes and Stan Sander (NASA-JPL) for allowing use of their UV- spectroscopic facilities, and to Nathan Dalleska (Caltech) for GC-MS analysis of OCS samples.

**References**

- Breckenridge, W.H., and H. Taube, Ultraviolet spectrum of carbonyl sulfide, *J. Chem. Phys.*, *52*, 1713-1715, 1970.
- Flothmann, H., C. Beck, R. Schinke, C. Woywood, and W. Domcke, Photodissociation of ozone in the Chappuis band. II Time-dependent wave-packet calculations and interpretation of diffuse vibrational structures, *J. Chem. Phys.*, *107*, 7296-7313, 1997.
- Gordus, A.A., and R.B. Bernstein, Isotope effect in continuous ultraviolet absorption spectra: methyl bromide-d<sub>2</sub> and chloroform-d, *J. Chem. Phys.*, *22*, 790, 1954.
- Griffith, D.W.T., G.C. Toon, B. Sen, J.F. Blavier, and R.A. Toth, Vertical profiles of nitrous oxide isotopomer fractionation measured in the stratosphere, *Geophys. Res. Lett.*, *27*, 2485-2488, 2000.
- Heller, E.J., The semiclassical way to molecular spectroscopy, *Acc. Chem. Res.*, *14*, 368-375, 1981.
- Herzberg, G., *Molecular Spectra and Molecular Structure*, p. 453 pp., van Nostrand, Princeton, N.J., 1966.
- Johnson, M.S., G.D. Billing, A. Gruodis, and M.H.M. Janssen, Photolysis of nitrous oxide isotopomers studied by time-dependent hermite propagation, *J. Phys. Chem. A*, *105*, 8672-8680, 2001.
- Kulander, K.C., C. Cerjan, and A.E. Orel, Time-dependent calculations of molecular photodissociation resonances, *J. Chem. Phys.*, *94*, 2571-2577, 1991.
- Leung, F.Y., A.J. Colussi, G.C. Toon, and M.R. Hoffmann, Isotopic fractionation of carbonyl sulfide in the atmosphere: Implications for the source of background stratospheric sulfate aerosol, *Geophys. Res. Lett.*, *10.1029/2001GL013955*, 2002.
- Miller, C.E., and Y.L. Yung, Photo-induced isotopic fractionation, *J. Geophys. Res.*, *105*, 29039-29051, 2000.
- Molina, L.T., J.J. Lamb, and M.J. Molina, Temperature dependent UV absorption cross sections for carbonyl sulfide, *Geophys. Res. Lett.*, *8*, 1008-1011, 1981.
- Pack, R.T., Simple theory of diffuse vibrational structure in continuous uv spectra of polyatomic molecules. I. Collinear photodissociation of symmetric triatomics, *J. Chem. Phys.*, *65*, 4765-4770, 1976.

- Rahn, T., H. Zhang, M. Wahlen, and G.A. Blake, Stable isotope fractionation during ultraviolet photolysis of N<sub>2</sub>O, *Geophys. Res. Lett.*, *25*, 4489-4492, 1998.
- Schinke, R., and V. Engel, Periodic orbits and diffuse structures in the photodissociation of symmetric triatomic molecules, *J. Chem. Phys.*, *93*, 3252-3257, 1990.
- Sugita, A., M. Mashino, M. Kawasaki, Y. Matsumi, B. R., G. Trott-Kriegeskorte, and K.-H. Gericke, Effect of molecular bending on the photodissociation of OCS, *J. Chem. Phys.*, *112*, 7095, 2000.
- Suzuki, T., H. Katayanagi, S. Nanbu, and M. Aoyagi, Nonadiabatic bending dissociation in 16 valence electron system OCS, *J. Chem. Phys.*, *109*, 5778, 1998.
- Turatti, F., D.W.T. Griffith, S.R. Wilson, M.B. Esler, T. Rahn, H. Zhang, and G.A. Blake, Positionally dependent N-15 fractionation factors in the UV photolysis of N<sub>2</sub>O determined by high resolution FTIR spectroscopy, *Geophys. Res. Lett.*, *27*, 2489-2492, 2000.
- Wu, C.Y.R., F.Z. Chen, and D.L. Judge, Temperature dependent photoabsorption cross sections of OCS in the 2000-2600 Å region, *J. Quant. Spectrosc. Radiat. Transfer*, *61*, 265-71, 1999.
- Zhang, H., P.O. Wennberg, V.H. Wu, and G.A. Blake, Fractionation of <sup>14</sup>N<sup>15</sup>N<sup>16</sup>O and <sup>15</sup>N<sup>14</sup>N<sup>16</sup>O during photolysis at 213 nm, *Geophys. Res. Lett.*, *27*, 2481-2484, 2000.